




Original Article

Surfacing and vertical behaviour of Atlantic bluefin tuna (*Thunnus thynnus*) in the Mediterranean Sea: implications for aerial surveys

Robert Klaus Bauer , Fabien Forget, Jean-Marc Fromentin, and Manuela Capello

IRD, MARBEC, Univ Montpellier, CNRS, Ifremer, IRD, Sète, France

*Corresponding author: tel: +33 4 99 57 32 57; e-mail: manuela.capello@ird.fr.

Bauer, R. K., Forget, F., Fromentin, J.-M., and Capello, M. Surfacing and vertical behaviour of Atlantic bluefin tuna (*Thunnus thynnus*) in the Mediterranean Sea: implications for aerial surveys. – ICES Journal of Marine Science, 77: 1979–1991.

Received 16 October 2019; revised 10 March 2020; accepted 14 April 2020; advance access publication 26 June 2020.

Atlantic bluefin tuna (*Thunnus thynnus*) (ABFT) frequently engage in surface basking and foraging behaviour that makes them detectable from afar. This behaviour is utilized for the development of fisheries-independent abundance indices based on aerial surveys, although changes in the surface-feeding dynamics of ABFT are not yet accounted for. We investigated the daytime surfacing behaviour of ABFT at different temporal and vertical resolutions based on 24 individuals (117–158 cm fork length), tagged with pop-up archival tags in the Gulf of Lion, NW-Mediterranean Sea between 2015 and 2016. The results suggest that ABFT remain usually <2 min continuously within the visible surface (0–1 m) during daytime. ABFT presence in the 0–1 and 0–20 m layers varied over time and between individuals but showed a seasonal decline towards autumn with the breakdown of thermal stratification. Furthermore, the rate of surfacing events was highly correlated with the time spent in the 0–20 m layer. Geolocation estimates confirm a strong site fidelity of ABFT during the aerial survey period (August–October) in the Gulf of Lion. Our results support the choice of the survey region and period, but related indices should account for the seasonality of ABFT surface behaviour [i.e. the time spent in the 0–20 m layer].

Keywords: abundance index, archival tags, surface availability, thermal stratification, vertical behaviour

Introduction

Atlantic bluefin tuna *Thunnus thynnus* (ABFT) are a highly migratory, opportunistic predators that can forage throughout the water column to depths >1000 m. Despite their physiological capabilities, ABFT prefer the epipelagic zone, where they frequently feed on schools of small epipelagic fish such as sardines and anchovies (Lutcavage and Kraus, 1997; Fromentin and Powers, 2005; Bauer *et al.*, 2017). This behaviour facilitates the detection of tuna schools from afar and led to the use of spotter planes in tuna purse-seine fisheries (Farrugio, 1977; Basson and Farley, 2014). Like fisherman, scientists also exploit the fact that ABFT are visible at the surface by conducting scientific aerial surveys to count tuna schools with the objective of obtaining a fisheries-independent abundance index. Several aerial surveys are conducted in different regions worldwide, such as in Australia on

southern bluefin tuna (*Thunnus maccoyii*; Eveson *et al.*, 2018) as well as on ABFT in the northwestern Mediterranean Sea (Fromentin, 2003; Bauer *et al.*, 2015a). Because variations in the vertical behaviour (i.e. changes in the “surface availability”) of tunas can significantly affect the number of schools observed at the sea surface (Bauer *et al.*, 2015c), accounting for this variability is a key step to provide a robust abundance index.

Several studies have sought to determine the factors driving the vertical behaviour of bluefin tuna (Walli *et al.*, 2009; Galuardi and Lutcavage, 2012; Marcek *et al.*, 2016; Bauer *et al.*, 2017; Eveson *et al.*, 2018). Archival tagging data from the Atlantic Ocean have demonstrated that the vertical behaviour of ABFT is influenced by the thermal stratification of the water column (Brill *et al.*, 2002; Walli *et al.*, 2009; Galuardi and Lutcavage, 2012). Similar relationships were demonstrated in other oceans for

Southern and Pacific Bluefin tuna (Kitagawa *et al.*, 2007; Eveson *et al.*, 2018). Recently, 24-h-depth frequency data from tagging studies conducted in the Gulf of Lion (northwestern Mediterranean Sea) showed that mature ABFT (124–255 cm fork length vs. 110–135 cm length at maturity Fromentin and Powers, 2005; Farley and Ohshimo, 2018) gradually moved from surface layers to deeper waters as winter approached and the waters became less stratified (Bauer *et al.*, 2017). These results confirmed the suitability of the aerial survey period (late summer–autumn) in this region to maximize the chances of observing ABFT schools at the sea surface. However, one of the main limitations of this study was the low resolution of the available data sets, mainly consisting of 24 h presence rates in predefined depth layers that impeded a fine-scale analysis of the vertical behaviour of ABFT and its drivers. Using high-resolution depth data (five individuals, 179–227 cm fork length) and a recovered Mk10 tag (160 cm fork length), Bauer *et al.* (2017) identified an inversion in the diel vertical behaviour in the Gulf of Lion area where aerial surveys were conducted, with higher presence rates between 0 and 10 m during the day in summer and during the night in winter. However, the significance of this depth layer for surfacing behaviour remained unclear, and the resolution of the available data was insufficient to provide an adequate estimate of the proportion of time spent in the visible surface layer (VSL) (0–1 m; surface availability), as a proxy of feeding behaviour and the duration of surfacing events.

Higher-resolution depth time series data are required to identify and explain changes of juvenile ABFT presence VSL (0–1 m; surface availability) and thus the related variability in the number of schools observed during subsequent aerial surveys. Like other near-coastal areas of high biological productivity, the Gulf of Lion has been identified as a key nursery ground for ABFT (Royer *et al.*, 2004; Druon *et al.*, 2011), where large quantities of maturing and adolescent ABFT (length at maturity is 110–135 cm; Fromentin and Powers, 2005; Farley and Ohshimo, 2018) are seen at the surface. Mature ABFT are also present in the area but less abundant and not participating in the surface foraging (Bauer *et al.*, 2015a).

Former tagging experiments in this region only yielded (few high-resolution) vertical behaviour data of mature ABFT (>160 cm fork length) because of the physical constraints of tagging with early pop-up archival tag models (Fromentin and Lopuszanski, 2014; Bauer *et al.*, 2015a, 2017). Accordingly, the horizontal movements and vertical dynamics of maturing and adolescent individuals, which constitute the majority of the tuna schools spotted by plane surveys, remain unknown. Filling this knowledge gap is a crucial step to characterize the surface availability of juveniles and improve abundance indices of ABFT from aerial surveys in the Gulf of Lion.

In the Atlantic Ocean, ABFT is managed by the International Commission for the Conservation of Atlantic Tunas (ICCAT). The regulatory measures adopted by ICCAT in the 2000s for the ABFT rebuilding plan have introduced extensive changes in the spatio-temporal patterns of the ABFT fisheries, thus significantly affecting the fisheries-dependent indices traditionally employed for the assessment of the eastern Atlantic and Mediterranean bluefin tuna stock (ICCAT, 2013; Fromentin *et al.*, 2014). Consequently, the ABFT stock assessment requires alternative abundance indices based on fisheries-independent data, as well as reliable methods for estimating the degree of confidence of such indices. In this respect, aerial surveys of ABFT schools, coupled to

novel assessment methodologies, are now considered vital alternatives to fisheries-based abundance estimates (Walli *et al.*, 2009; Bonhommeau *et al.*, 2010).

In this study, we investigated the surfacing behaviour of ABFT (117–158 cm fork length) based on high-resolution electronic tagging data collected during the aerial survey season in the Gulf of Lion (northwestern Mediterranean Sea). Our objectives were to (i) quantify and compare potential indicators of juvenile ABFT daytime surfacing behaviour based on different temporal resolutions and depth layers, (ii) identify related temporal patterns, (iii) characterize the environmental factors that can drive these patterns, and (iv) address the relevance of these indicators for the design and correction of ABFT aerial surveys.

Material and methods

Tag programming

To study ABFT behaviour, we used miniPATs, pop-up satellite archival tags (PSATs) by Wildlife Computers (<https://wildlife.computers.com>). These tags can record depth and temperature time series (denoted below as DepthTS and TempTS, respectively) at a temporal resolution of 3–5 s (depending on the predefined deployment duration) and a vertical resolution of 0.5 m. Based on these data, the tag calculates and stores additional data products such as PAT-style Depth–Temperature profiles (PDT), time at depth data, and time at temperature (Wildlife Computers, 2016). After pop-up, the tags transmit user-defined data products and subsets from the recorded data sets. All our tags were configured to transmit the following data products: daily light curves, DepthTS, and PDT. In order to maximize data coverage of the transmitted datasets, we decreased the temporal resolution of the DepthTS and PDT data after the first tagging campaign in 2015 from 150 to 600 s and 6 to 24 h, respectively (Table 1). For both years, deployment durations were set to 150 and 90 d during spring (April–May) and summer (August–September), respectively, in order to cover the aerial survey period in the Gulf of Lion (August–October).

Electronic tagging

Electronic tagging operations were conducted during two periods: August–September 2015 and April–September 2016. Tagging trips were conducted during these specific temporal windows in order to target ABFT in the study area.

Tunas were caught on rod and reel using bait and artificial lures on board sport fishing vessels. Captured ABFT were carefully landed onto a wet vinyl mat, where their eyes were immediately covered with a wet cloth and their gills continuously irrigated by placing a hose pumping seawater in the fish's mouth. The hook was then removed and the fork length (FL) measured. Only ABFT individuals in good condition (e.g. without any previous injuries) with a preferred fork length between 110 and 160 cm were tagged. The miniPATs (Wildlife Computers, <https://wildlife.computers.com>) were rigged with a 12-cm stainless steel cable and a large Domeier anchor. The tags were inserted at the base of the second dorsal fin, between the pterygiophores using a stainless steel applicator. A keeper strap was used to immobilize the tag by placing an additional plastic anchor, ~20 cm towards the caudal end of the first anchor. Prior to use, tethers, tag applicators, and anchors were disinfected with an 8% povidone-iodine solution (Betadine). After tagging, the fish were released head first back into the sea and the deployment location and time noted. A social

Table 1. Tag deployments metadata for the 24 pop-up archival tags deployed during 2015 (n = 6) and 2016 (n = 18) in the Gulf of Lions, France.

#	Tag ID	Deployment			Release			Days at liberty	DepthTS resolution (s)	TS resolution (s)	Set
		Fork length (cm)	Date	Latitude	Longitude	Date	Latitude				
1	14P0818	127	2015-08-05 06:48	43.24	4.84	2015-09-09 17:40	8.61	600	3	Recovered	
2	14P0814	144	2015-08-05 14:15	43.24	4.84	2015-09-27 12:00	6.43	600	600	Transmitted	
3	14P0813	131	2015-09-10 09:24	43.25	4.87	2015-10-25 20:00	4.93	600	600	Transmitted	
4	14P0824	130	2015-09-10 09:55	43.25	4.87	2015-10-25 22:20	4.18	600	3	Recovered	
5	14P0825	140	2015-09-25 09:00	43.25	5.12	2015-11-14 20:00	4.97	150	150	Transmitted	
6	14P0821	141	2015-09-25 11:45	43.25	5.12	2015-11-08 02:37	4.76	150	150	Transmitted	
7	14P0823	120	2016-04-17 10:57	42.43	3.27	2016-09-11 12:10	13.51	600	600	Transmitted	
8	14P0819	117	2016-04-17 12:57	42.4	3.26	2016-09-15 15:45	3.13	600	600	Transmitted	
9	14P0815*	129	2016-04-22 07:45	42.66	3.1	2016-05-04 11:46	3.42	300	5	Recovered	
10	14P0816	132	2016-04-22 09:51	42.69	3.08	2016-05-30 07:00	2.95	600	600	Transmitted	
11	15P0986*	140	2016-08-03 08:55	43.14	5.2	2016-08-09 18:50	6.72	300	300	Transmitted	
12	15P0983*	146	2016-08-03 12:00	43.14	5.2	2016-08-06 17:00	5.1	300	300	Transmitted	
13	15P0985*	156	2016-08-03 12:25	43.14	5.2	2016-08-05 13:15	5.08	300	300	Transmitted	
14	15P1019*	146	2016-08-07 08:00	43.13	5.2	2016-08-19 18:05	4.68	300	300	Transmitted	
15	15P1022	153	2016-08-07 14:45	43.13	5.2	2016-09-03 17:20	4.93	600	600	Transmitted	
16	11P0584	142	2016-08-25 08:30	43.14	5.18	2016-11-23 21:54	5.01	600	5	Recovered	
17	11P0587	144	2016-08-26 12:50	43.14	5.16	2016-11-24 22:10	5.05	600	600	Transmitted	
18	11P0279	147	2016-08-26 13:39	43.14	5.16	2016-09-29 12:00	4.74	600	600	Transmitted	
19	13P0243	147	2016-08-26 14:36	43.15	5.16	2016-11-16 00:30	6.75	600	3	Recovered	
20	15P1025	125	2016-08-28 08:40	43.23	4.77	2016-11-26 20:00	3.9	600	600	Transmitted	
21	15P0984	158	2016-08-28 15:00	43.23	4.23	2016-10-19 14:01	4.37	600	3	Recovered	
22	15P1023	128	2016-08-31 10:00	43.23	4.74	2016-09-19 15:00	4.79	600	600	Transmitted	
23	15P1024	135	2016-08-31 11:00	43.23	4.74	2016-10-16 01:01	4.55	600	3	Recovered	
24	15P1016	130	2016-08-31 12:30	43.23	4.74	2016-10-12 12:20	8.57	600	600	Transmitted	

The * symbol indicates prematurely released tags with deployment durations of <15 d that transmitted DepthTS at 300-s resolution unless the originally programmed resolution was higher.

media campaign (<https://www.facebook.com/marine.biologging>) was initiated after the 2016 tagging campaign to increase the chance of tag recovery.

Data analysis

Geolocation estimates

The tagging data were automatically uploaded to the Wildlife Computers Data Portal (<http://my.wildlifecomputers.com/data/>). For all tags, geolocations were processed using Wildlife Computer GPE3 algorithm, which is available on the data portal (Wildlife Computers, 2015). This algorithm is based on a gridded hidden Markov model, which incorporates light level and sea surface temperature (SST) data of the tags as well as SST (Reynolds *et al.*, 2002) and bathymetry reference data (NOAA ETOP01 global relief model, Bedrock version through the R-package “oceanmap” Amante and Eakins, 2009; Bauer, 2019). Additional model inputs included the tag deployment and pop-up locations/times as well as an estimate of the typical travelling speed of the tagged animal. For the tag pop-up location, we used the first ARGOS location estimates transmitted (class 1–3; Service Argos Inc, 2005). In contrast, transmitted and (when available) recovered DepthTS data were used to estimate the tags’ time of release (last DepthTS time record prior to pop-up and transmission start). Different travelling speeds (2.1, 3.1, and 4.1 km h⁻¹) were tested, in accordance with available literature values (Wardle *et al.*, 1989; Lutcavage *et al.*, 2000). The selection of the optimal speed was done based on a model score produced by the GPE3 software, with higher scores of the Akaike information criterion (AIC) indicating better fits to the observed data. Model outputs included maximum likelihood tracks as well as the different likelihood areas (50, 80, 95, and 99%) for the animal position (Wildlife Computers, 2015). The maximum likelihood tracks were used to assess the residency of ABFT in the study region and their habitat utilization based on kernel densities that were generated with the *kde2d*-function of the “MASS” R-package (Venables and Ripley, 2002).

Environmental data

Three major indicators for the thermal-structure of the water column were estimated using the sensor data of the miniPATs: daily thermocline depth, thermocline gradient as well as the thermal stratification index, following the approach used by Bauer *et al.* (2015b) implemented in the R-package “RchivalTag” (Bauer, 2018). To do so, PDT or, when available, recovered Depth–Temperature time series data were used (see Supplementary material for detailed description). A comparative analysis on the accuracy of the three indicators obtained from PDT and Depth–Temperature time series data from the recovered tags (Supplementary Figure S1) revealed that the stratification index was particularly robust for days when the vertical profile of the tagged individuals was ≥ 88 m. We therefore estimated the stratification index from PDT profiles or (if available) recovered Depth–Temperature time series data that met this requirement in the subsequent analyses. Missing values in the time series of the stratification index were estimated by applying an exact cubic regression spline, using the function “*spline*” of the standard R-package “*stats*” (Forsythe *et al.*, 1977; R Core Team, 2017).

Vertical behaviour

The analysis of ABFT vertical behaviour focused on daytime DepthTS data from the Gulf of Lion region that is most relevant for the aerial surveys (Bauer *et al.*, 2015a), see Figure 1. For this purpose, we selected only DepthTS data recorded between the time of sunrise and sunset, whose corresponding daily position estimates were located within 3–6°E and 41.5–44°N. To account for temporal and regional changes in the timing of sunrise and sunset during the deployment periods, we estimated the timing of both events per day and tag by applying the function “*get_DayTimeLimits*” of the R-package “*RchivalTag*” (Bauer, 2018). Only complete daily DepthTS (i.e. DepthTS without any transmission gaps during daytime) were considered in the subsequent analyses. For the physically recovered tags, the entire DepthTS recorded at resolutions of 3–5 s within the study region could be used for the analysis.

Because we obtained DepthTS data in different resolutions (high-resolution data for the recovered tags and 600-s resolution DepthTS for all the remaining tags), the analysis of vertical behaviour of ABFT was structured over two different temporal scales. First, we characterized the vertical behaviour of ABFT through the combined 600-s DepthTS datasets from the unrecovered (but transmitted) DepthTS data as well as the recovered tagging data, the latter being resampled at 600 s to ensure homogeneity among datasets. Then, a fine-scale analysis was conducted from the high-resolution recovered tags, considering a common resolution of 15 s, by subsampling the 3–5 s resolution data for all the recovered tags. Finally, using the recovered tags, we studied the relation between the fine-scale behaviour characterized at a resolution of 15 s and the occupation of the water column obtained at 600-s resolution.

Vertical behaviour—all tags (600-s resolution)

We analysed the monthly daytime presence rate of ABFT at different depths based on the merged data sets of 2015 and 2016. We estimated the monthly average proportion of time that ABFT spent within different depth bins (0, 10, 20, 50, 200, 300, 400, 600, 1000, and >1000 m) during daytime as well as its standard deviation from the related daily data of each individual. The temporal evolution of daytime presence in the 0–20 m layer (named near-surface layer, NSL) was further analysed based on the daily average of individual daytime presence rates in the 0–20 m layer (named NSL). Daily presence rates were estimated for each tagged individual considering the percentage of vertical positions located within the NSL layer during daytime. Daily presence rates were averaged and their standard deviation estimated over different individuals present during the same day in the study region. The same analysis was conducted for the 0–10 m layer, see the Supplementary Material.

Fine-scale vertical behaviour—recovered tags (15- and 600-s resolution)

The fine-scale analysis of vertical behaviour of ABFT focused on the time spent in the 0–1 m layer, termed VSL, as a proxy for surface availability. We therefore estimated daily presence rates of ABFT in the VSL with the same procedure as used to estimate daily average presence rates in the NSL (see section “Vertical behaviour—all tags (600-s resolution)”). We then calculated the continuous bouts of time spent by each individual within a given depth layer. This approach has been used to estimate residence

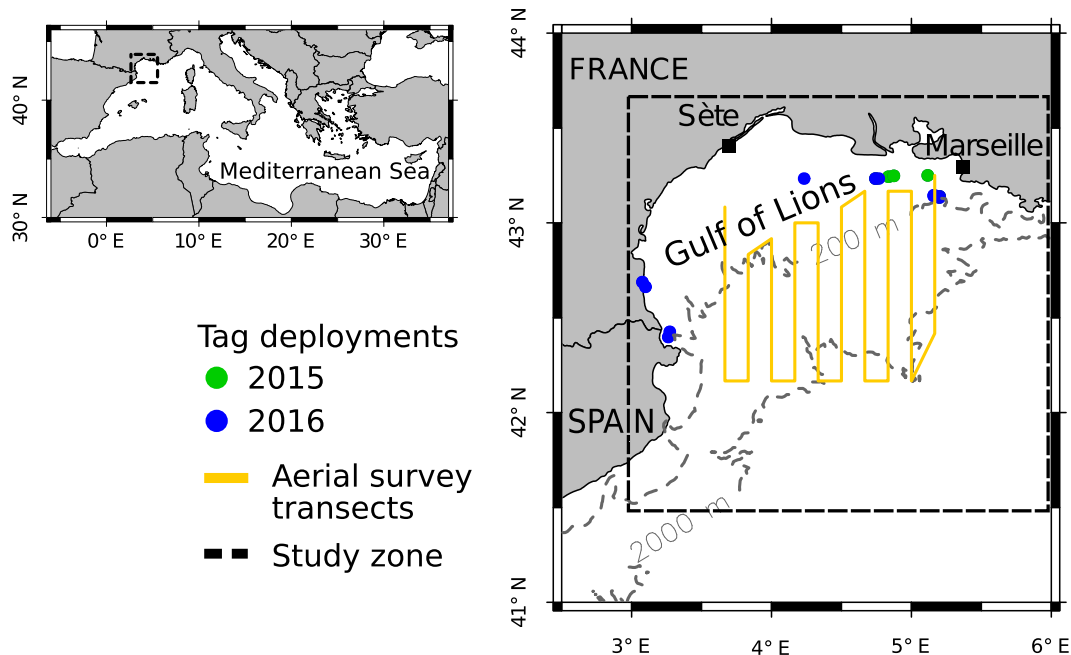


Figure 1. The Gulf of Lions, North Western Mediterranean Sea. The green and blue dots indicate the tag deployment locations for year 2015 and 2016, respectively, and the yellow lines show the aerial survey transects. The dotted black rectangle denotes the study area. Maps were generated using the “plotmap”-functions of the R-package “oceanmap” (Bauer, 2019).

and absence times for acoustically tagged individuals around instrumented sites (Robert *et al.*, 2013; Capello *et al.*, 2015). Each time an ABFT individual was present within the same depth layer, its continuous residence time (CRT) was incremented by an amount of time corresponding to the temporal resolution of the data. In contrast, if ABFT moved out of the layer, the respective CRTs ended. Following this definition, the CRTs recorded for the VSL (0–1 m), named CRT_{VSL} , were estimated.

Because the surface availability of individual ABFT could differ to that of tuna schools, we aimed at calculating the CRT of tuna schools in the VSL (called CRT_{VSL}^{school}) as a proxy of the school visibility from an aeroplane. A feeding tuna school can be interpreted as the sum of feeding individuals, both tagged and non-tagged. In such an event, single individuals may dive below the VSL, whereas others remain inside so that the entire school remains visible for a longer period than the tagged individual. To account for this, we considered that if a tagged individual was present in the VSL, with time gaps smaller than $\Delta t = 1$ min, the school was still visible at the surface and its CRT_{VSL}^{school} incremented. Conversely, if the tagged individuals left the VSL layer for a time interval larger than Δt , the duration of the respective CRT_{VSL}^{school} is ended. The idea of adding a time gap Δt is similar to the concept of maximum blanking period (MBP, Capello *et al.* 2015), where brief absences, below a given threshold (the MBP), are not accounted in the CRT estimates, namely the school is considered to still be present in this layer.

Given that both high-resolution data from recovered tags and transmitted lower-resolution data were available, we tested how the time series data at high resolution (15 s) translates into lower-resolution data sets (600 s). We therefore considered, for each position of a recovered tag in the 0–1 m layer at time t , two random vertical positions at time $t - \alpha$ and $t - \alpha + 600$ s, with α being a

random number sampled over the set of discrete values $\{15$ s, 30 s, 45 s, \dots , 600 s $\}$. We then drew the cumulative curve on the frequency of these vertical positions to obtain the occupation rates of different depths within the 600-s interval around the surfacing events of ABFT. Moreover, we estimated the CRTs in the NSL (CRT_{NSL} , 0–20 m) and the deep layer (CRT_{DL} , >20 m) based on the subsampled 600-s recovered-tag data sets. Figure 2 provides a schematic view of the different CRTs used to characterize to the vertical behaviour of ABFT and Supplementary Table S1 resumes the resolution used to estimate the CRTs for each layer.

The similarity between CRTs of different layers was tested per month using the Kruskal–Wallis test of comparison, using the “kruskal.test” of the R-package “stats” (R Core Team, 2017). Finally, Pearson’s product–moment correlation coefficients were calculated using the function “cor” of the R-package “stats” (R Core Team, 2017) to investigate the correlation between the number of surfacing events (i.e. the number of CRT_{VSL}) and the time spent in the 0–20 m layer (i.e. the duration of the CRT_{NSL}).

Results

Tagging data

A total of 24 tags were deployed between 2015 and 2016 mainly maturing and adolescent ABFT (117–158 cm fork length; Table 1). Only 8 of the 24 tags remained attached to the fish until the end of their intended deployment period (90–150 d). Actual deployment durations ranged from 2 to 151 d with an average of 50.8 d \pm 40.2 SD (Figure 3). Three tags from 2016 had deployment durations of <1 week (#15P0983, #15P0985, and #15P0986) because of hardware failure. In addition, two tags (#14P0821 and #14P0825) from the 2015 tagging trip provided only 1–4 d of complete DepthTS data, despite rather short

deployment durations of 44–51 d, because of the specific tag configuration applied. DepthTS data from these five tags were not used in the subsequent analyses. Out of the 24 deployed tags, seven were physically recovered (Table 1), providing the complete

archived time series data at a resolution of 3–5 s. Nineteen tags provided more than 7 d of complete DepthTS data (i.e. without transmission gaps) (Table 1 and Supplementary Table S2).

Residency in the Gulf of Lion

The tracks obtained using a speed of 4.1 km h⁻¹ in the GPE3 model performed generally better than the 2.1 and 3.1 km h⁻¹ models, both on transmitted and recovered datasets (Supplementary Table S3). Only tag 15P0983 showed a better performance of the 2.1 km h⁻¹ model. Based on the maximum likelihood tracks, the study zone encompassed the high density area of the tags' geolocations (Figure 4) corresponding to 63.5% of all tag geolocations recorded during both years (Figure 3 and Supplementary Figure S2). Fish tagged since August in 2016 showed a higher residency in the study area than those tagged during the same period in 2015, accounting 80.5% (± 21.0 SD) vs. 51.8% (± 37.4 SD) on average, respectively. In fact, 13 of 14 ABFT tagged during August 2016 spent >50% and 5 of them 100% of the time in the Gulf of Lion. In contrast, only two out of the six ABFT tagged in 2015 showed a similar preference and remained the entire deployment period of their tag (45–46 d) in the Gulf of Lions. All four ABFT tagged during the spring season (end of April 2016) left the Gulf of Lion shortly after tagging for at least 1 month. Only two of these fish kept their tag until mid-September (the intended end of deployment) and returned twice to the Gulf of Lion during this period (Figure 3 and Supplementary Figure S2). No tagged tuna left the Mediterranean Sea towards the Atlantic and only one fish left the western Mediterranean during the study (Figure 4 and Supplementary Figure S2). This fish (#14P0823) was tagged during spring 2016

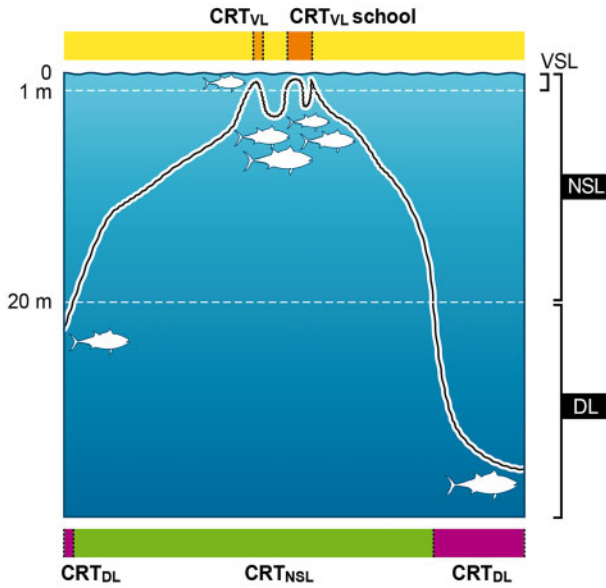


Figure 2. Schematic illustration of the three different depth layers (VSL: visual surface layer; NSL: near-surface layer; DL: deep layer) and related CRT examples of individual fish and tuna schools that were used to study the vertical behaviour of ABFT.

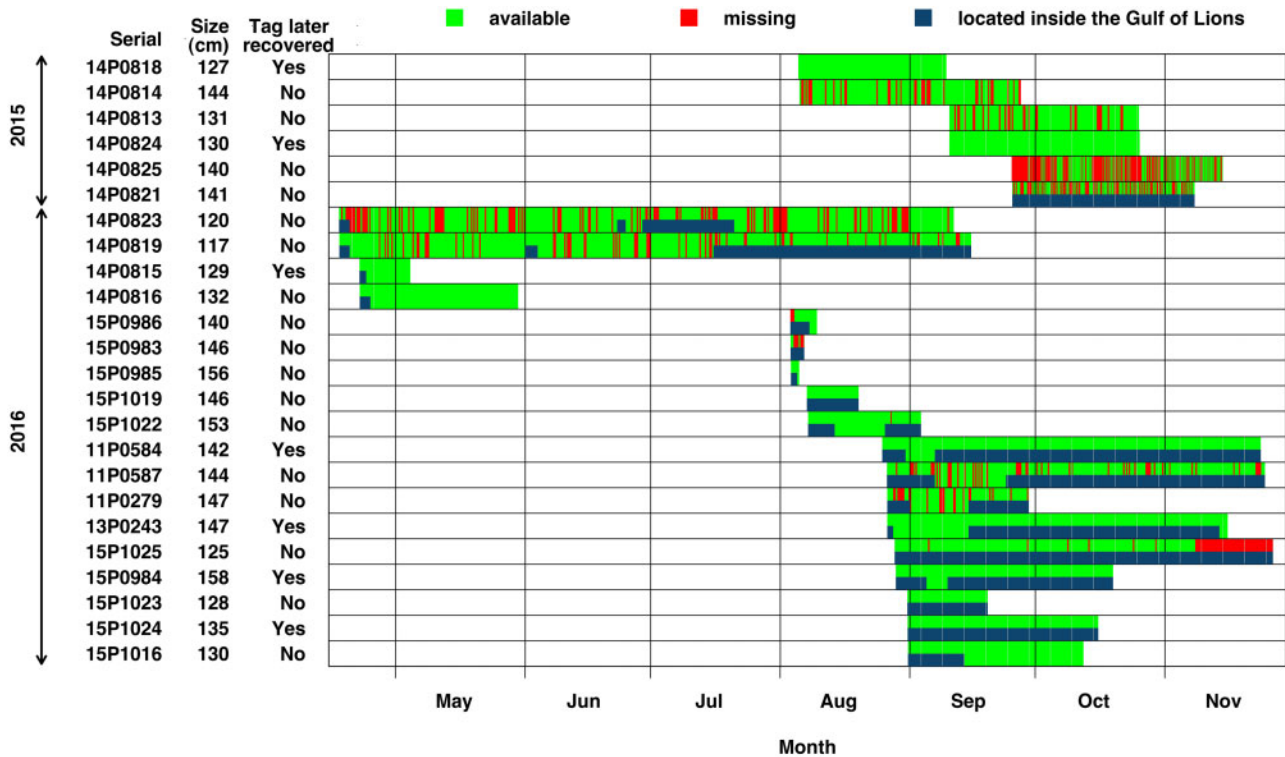


Figure 3. Temporal coverage (green) of DepthTS data per deployed tag. Data gaps because of transmission loss are shown in red. Blue bars indicate the periods spent inside the study area of the Gulf of Lions. Bold serial numbers indicate tagging data used in the analyses.

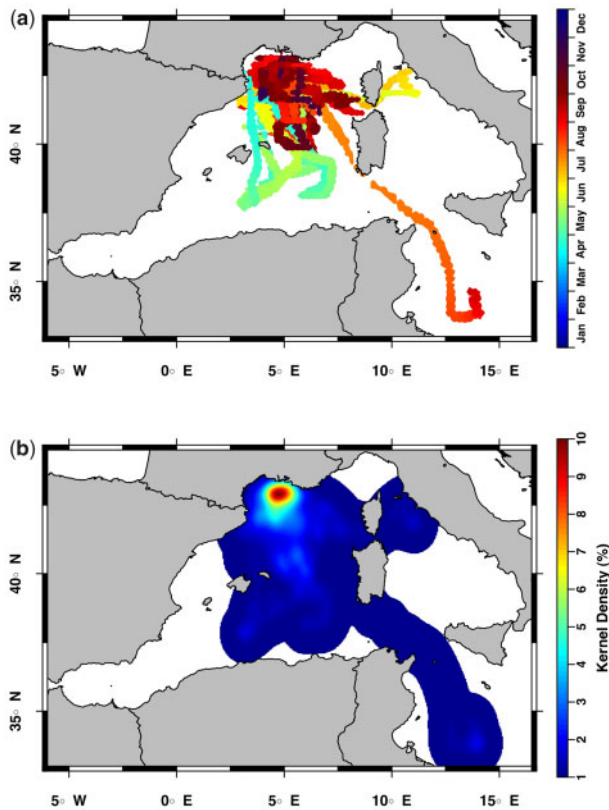


Figure 4. (a) 80% surface probability maps for each tag based on the most likely of the assumed travel speeds. (b) Combined kernel densities of all tags deployed during 2015 and 2016. Maps were generated using the “plotmap”- and “v”-functions of the R-package “oceanmap” (Bauer, 2019). For individual tracks, see [Supplementary Figure S2](#).

and ultimately moved to the Eastern Mediterranean basin, where the tag surfaced between Malta and Libya.

Vertical behaviour from all tags

Monthly presence rates in the water column

The proportion of time spent by ABFT at different depth strata showed a clear temporal trend (Figure 5). The occupation of the 0–10 m depths increased from spring (April) to summer (July), remained stable during July–September and then decreased in autumn (October), attaining the lowest values in November. The occupation of the depths between 10 and 20 m was less pronounced and did not show clear temporal changes, whereas the depths below 20 m showed an opposite trend relative to the 0–10 m, with the time at depth first decreasing from spring to summer, then increasing from summer to autumn.

Time series of daily presence rates in the NSL

For both 2015 and 2016, the daily presence rates of ABFT in the NSL (0–20 m) attained maximum values (>90%) during the summer (July–September) and showed a sharp decrease between September and October (Figure 6), in parallel with the decline of the thermal stratification index. The sensitivity analysis with a more restrictive NSL (0–10 m) revealed a similar trend and

relationship to the thermal destratification ([Supplementary Figure S3](#)).

Fine-scale vertical behaviour from recovered tags

Six of the seven recovered tags were present in the study zone during the period August–October (Figure 2). We therefore focused the high-resolution data analyses on this dataset during both study years, 2015 and 2016.

Surface availability: presence rates and duration of residency in the VSL

The daily presence rates of the seven recovered tags within the 0–1 m layer (VSL) showed during both years a high variability over time and between individuals, generally ranging between 0 and 60% apart from few extreme values (>80%) attained during August of both years (Figure 7). Presence rates in the VSL decreased from summer to autumn, in parallel with the decline of the thermal stratification index. This simultaneous decline was particularly visible in October 2016, when the presence rates and thermal stratification index both dropped abruptly.

The average time spent continuously in the 0–1 m layer (CRT_{VSL}) ranged between 1 and 2 min (Table 2). Although, there was no clear temporal trend (Figure 8), pairwise Kruskal–Wallis tests demonstrated significant differences in the average CRT_{VSL} between months and years ($p < 0.05$), except for September and October in 2016. Similarly, daily average durations of CRT_{VSL} demonstrated a high temporal variability for both years and no clear temporal trends ([Supplementary Figure S4](#)).

The estimated time that ABFT schools spent continuously at the surface (CRT_{VSL}^{school}), ranged between 3 and 6 min during all months of the study period (Table 2). Overall, the duration of CRT_{VSL}^{school} were longer than that of CRT_{VSL} , indicating that subsequent surfacing events occurred. The Kruskal–Wallis test of comparison on the monthly CRT_{VSL}^{school} demonstrated that there were significant ($p < 0.05$) differences between years and months (except for August and October in 2015), but no clear temporal trends were found (Figure 8 and [Supplementary Figure S4](#)).

Presence at other depth layers recorded at lower resolutions

The analysis of ABFT presence in the VSL relative to that of other depth layers revealed that >90% of all depth records within a temporal window of 600 s around individual surfacing events were located between 0 and 20 m (Figure 9).

During both years, the time spent continuously in the 0–20 m layer (CRT_{NSL}) was significantly different over different months (Kruskal–Wallis test, $p < 0.05$), except for August and September in 2015 (Figure 10 and Table 2). In 2015, the average CRT_{NSL} ranged between 1.9 (September) and 0.5 h (October). In 2016, the average CRT_{NSL} values ranged between 2.6 (August) and 0.9 h (October). A decreasing temporal trend in CRT_{NSL} towards October was particularly clear in 2016, both on a monthly and daily basis (Figure 10 and [Supplementary Figure S5](#)).

The average residence times in the Deep Layer (>20 m, CRT_{DL}) showed opposite trends to that of the NSL. Accordingly, the CRT_{DL} increased towards October, accounting 0.9 and 1.1 h in 2015 and 2016, respectively (Table 2, Figure 10, and [Supplementary Figure S5](#)). Minimum monthly average values of 0.3 and 0.4 h for the CRT_{DL} were recorded during September (2015) and August (2016), respectively. Pairwise Kruskal–Wallis tests demonstrated significant differences in the average CRT_{DL}

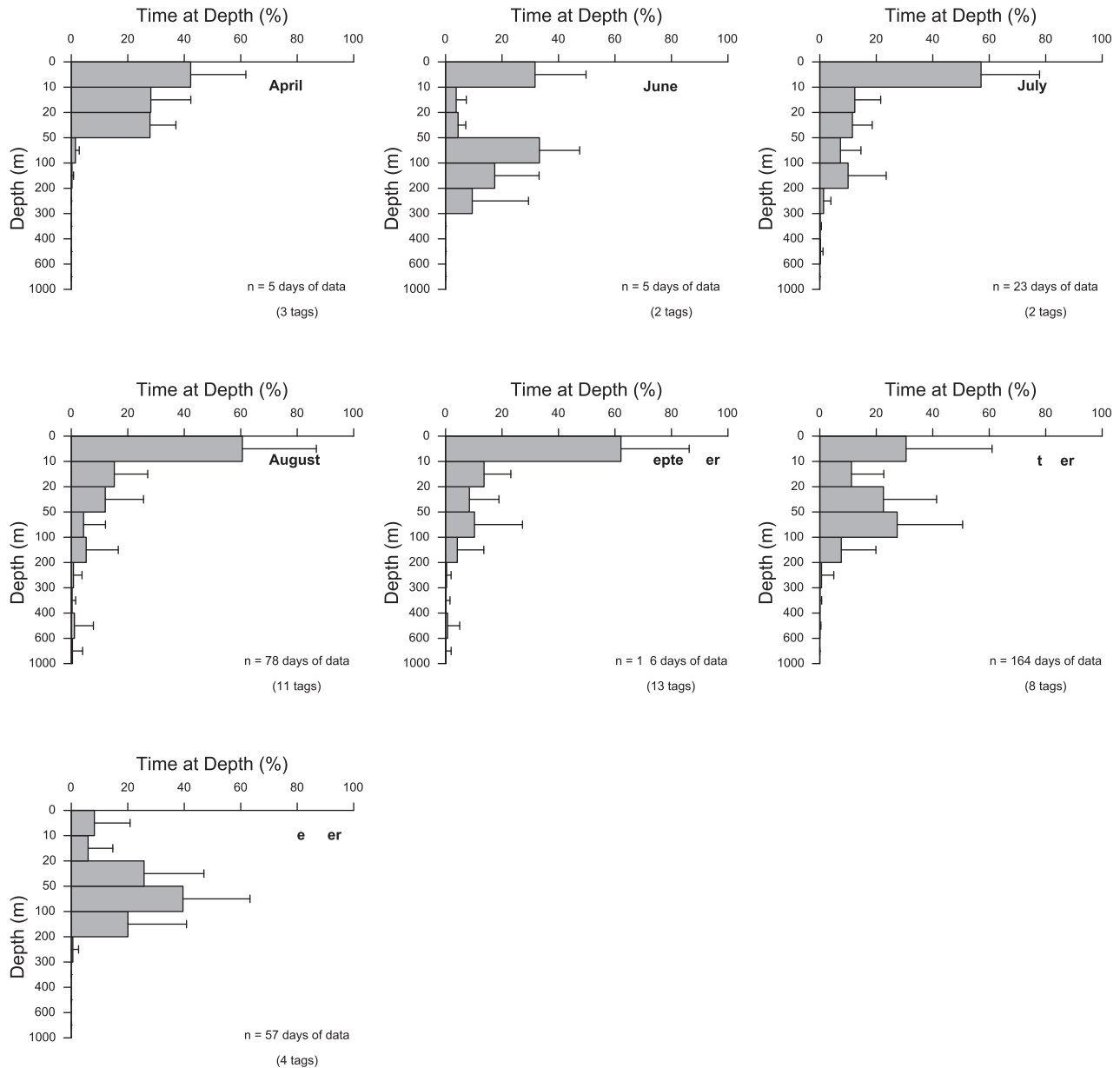


Figure 5. Average monthly percentages of the time at depth and its standard deviation (error bars) obtained from the daytime DepthTS data of all tags at 600-s resolution. Histograms were generated using the “hist_tad”-function of the R-package “RchivalTag” (Bauer, 2018).

between months and years ($p < 0.05$), except for August and September in 2015 and 2016.

The sensitivity analysis with a more restrictive NSL (0–10 m) and therefore larger DL (> 10 m) revealed similar trends in the average residence times (Supplementary Table S4 and Figures S6 and S7) and test results of monthly comparisons, although absolute estimates were of a smaller magnitude.

Correlation between subsequent CRTs, surface events, and time spent in the 0–20 m layer

Subsequent CRTs were weakly correlated irrespective of the reference layer and showed no apparent relationship. Accordingly, Pearson’s product–moment correlation coefficients of subsequent

CRTs in the VSL accounted 0.28 and 0.31 for individual tunas and tuna schools, respectively. Similarly, the correlation coefficients of subsequent CRTs in the NSL and DL accounted for 0.16 and 0.19, respectively.

In contrast, CRT durations of individual tunas in the NSL were highly correlated to the number of surface events (Figure 11 and Supplementary Figure S8). On a monthly basis, correlation coefficients between the daily CRT_{NSL} durations of the recovered tags and the respective number of surface events accounted for 0.81, 0.69, and 0.89, from August to October, respectively. The corresponding data of the tuna schools showed a constant increase in the linear correlation between the CRT durations in the NSL and number of school surface events from August to October, accounting for 0.68, 0.85, and 0.93.

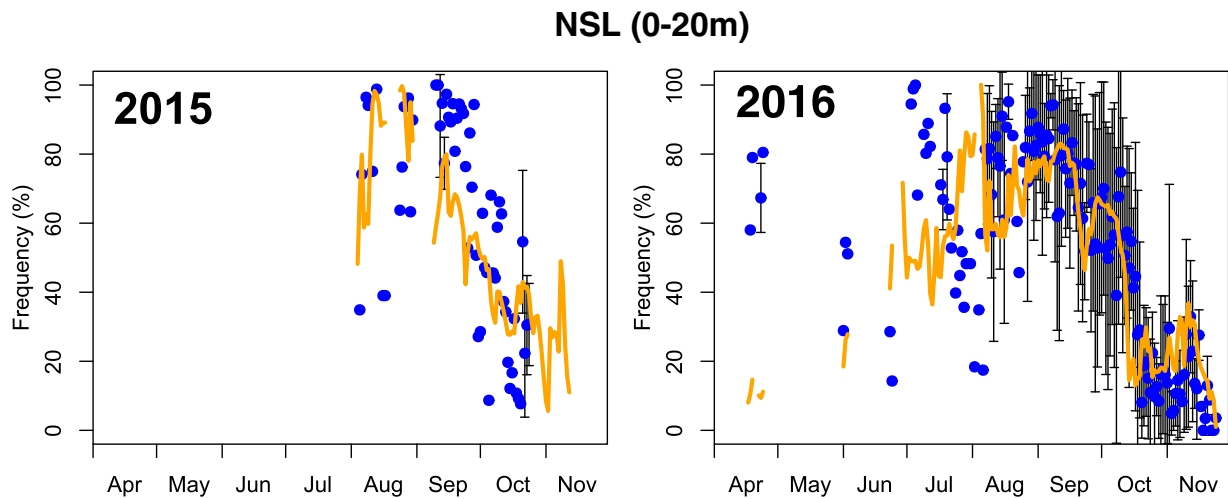


Figure 6. Average daily presence rates recorded in the 0–20 m depth layer (NSL) from all tags (blue dots) and its standard deviation (error bars) as well as the thermal stratification index (orange) in 2015 (left) and 2016 (right).

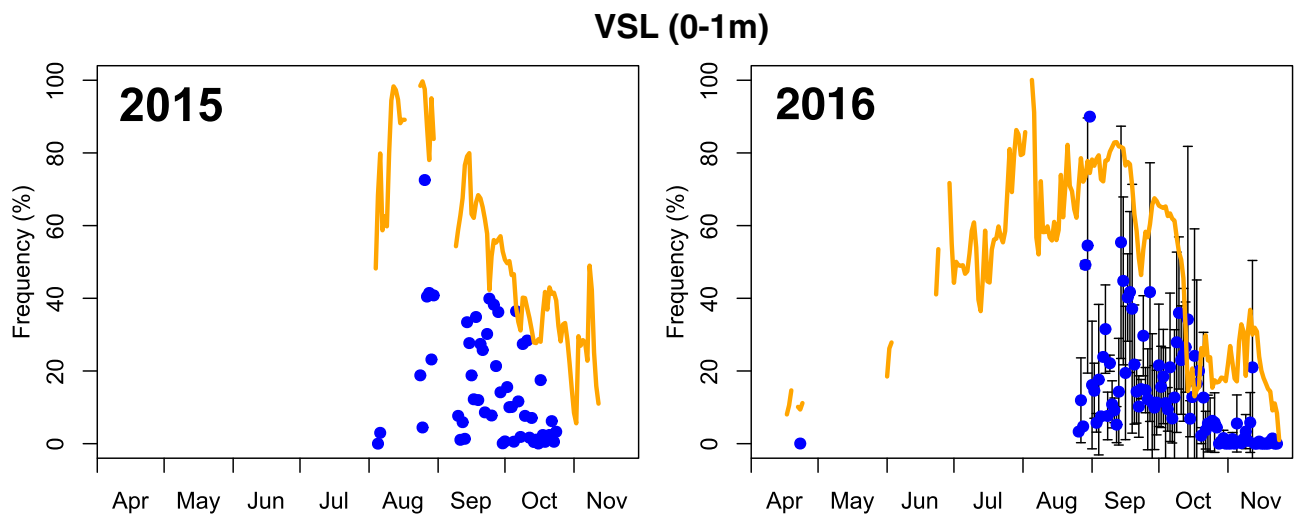


Figure 7. Average daily presence rates recorded in the 0–1 m depth layer (VSL) for the recovered tags (blue dots) and its standard deviation (error bars) as well as the thermal stratification index (orange) in 2015 (left) and 2016 (right).

Discussion

In this study, we investigated the site fidelity and vertical behaviour of maturing and adolescent ABFT in the Gulf of Lion. Compared with previous electronic tagging studies conducted in the same region (Fromentin and Lopuszanski, 2014), our study focused on smaller individuals (FL < 160 cm). The ABFT individual size ranges considered in this study (117–158 cm FL) are commonly found in the study region and are thus highly relevant for aerial surveys. However, so far there was no knowledge on their vertical behaviour and site fidelity.

This study demonstrated that the majority of the tagged tuna spent a large proportion of time within the Gulf of Lion, where they were tagged, in particular during the aerial survey season (August–October). This result is consistent with what was previously found for mature ABFT individuals (Fromentin and Lopuszanski, 2014). The consistency of the site fidelity of ABFT along different size ranges and years is highly relevant for the robustness of the abundance indices obtained through aerial

surveys. Namely, our results indicate that variabilities in the size distribution of ABFT individuals will not affect the indices.

The analysis of the monthly time at depth profiles demonstrated a strong seasonal pattern in the ABFT vertical behaviour, consistent with the findings of previous multiyear PSAT tagging studies conducted on larger individuals (Bauer *et al.*, 2017). The optimized deployment periods and transmission settings chosen allowed us to obtain complete depth time series and allowed the characterization of the vertical behaviour of multiple individuals on a daily basis. In this respect, the temporal evolution of daily presence rates of ABFT in the NSL (0–20 m) showed a seasonal trend that followed the thermal destratification of the water column, with high presence rates in the summer, where tuna spent up to 80–90% of the time in 0–20 m layer. Remarkably, the daily presence rates in the NSL showed a high variability, even among consecutive days. Moreover, large daily standard deviations were estimated over different individuals, thus revealing a high variability in the ABFT vertical behaviour, both at the intra and inter-

individual level. Such variability may be related to local environmental conditions, local availability of prey, or to the physiology of ABFT themselves. Marcek *et al.* (2016) showed that juvenile ABFT in the west-Atlantic Ocean apparently spent more time below the thermocline with increasing lunar illumination during night-time, but not during daytime. It is further noteworthy to recall that surface presence of ABFT is composed of various behavioural types, including foraging behaviour and horizontal migrations (Lutcavage and Kraus, 1997). Future studies could explain our findings through the use of new-generation tags that can measure the physiology and vertical behaviour of tagged individuals at the same time.

Table 2. Monthly average of daytime CRT_{VSL} , CRT_{VSL}^{school} , CRT_{NSL} and CRT_{DL} recorded for the recovered tags.

Year	Month	CRT_{VSL} (min)	CRT_{VSL}^{school} (min)	CRT_{NSL} (h)	CRT_{DL} (h)
2015	August	2.1 (4.2)	5.7 (21.8)	1.6 (2.2)	0.6 (1)
2015	September	1.1 (1.5)	3.5 (6)	1.9 (2.7)	0.3 (0.4)
2015	October	2.2 (3.7)	4.9 (8.4)	0.5 (0.5)	0.9 (1.1)
2016	August	1.7 (5.9)	4.6 (16.8)	3.9 (4.5)	0.3 (0.2)
2016	September	1.9 (4.7)	4.7 (13.4)	1.1 (1.9)	0.5 (0.9)
2016	October	1.5 (3.7)	4.1 (8.8)	1 (2.1)	1.4 (2.2)

Values in parentheses report the standard deviation. The corresponding results for a more restrictive NSL (0–10 m) and therefore larger DL (>10 m) are illustrated in [Supplementary Table S4](#).

Remarkably, during aerial surveys conducted over consecutive weeks or even days, it is not uncommon to encounter a similar degree of variability in the number of tuna schools spotted by the plane. In this respect, the high degree of inter-individual and temporal variability found in this study suggests that changes in the visibility conditions because of the sea state (i.e. waves vs. flat surface) constitute only one of the components of the system's variability.

From the 24 tags deployed, seven (29.1%) tags were recovered. The high resolution of the depth sensors of the tags (vertical resolution: 0.5 m; accuracy $\pm 1\%$) and the high temporal resolution of the recovered tags (<5 s) allowed the first in-depth analysis of ABFT vertical behaviour in the study region. For this purpose, surfacing events, identified through the presence of recovered tags in the VSL (0–1 m), were taken as a proxy for surface feeding. Our results showed that despite a high variability over time and between individuals, the presence in the VSL clearly dropped during October, following the decline of the thermal stratification index from summer to autumn. On the other hand, monthly and daily averaged CRTs in the VSL showed no such trend or seasonality. On average, CRTs of individual ABFT and tuna schools in the VSL lasted 1–2 min for all months, which is comparable with what was expected from boat-based observations of surfacing ABFT during tagging trips. School-related CRTs in the VSL were longer than that of individuals (3–6 min), indicating that subsequent surfacing events occurred.

The analysis of the high-resolution DepthTS data of the recovered tags allowed us to link different temporal and spatial scales.

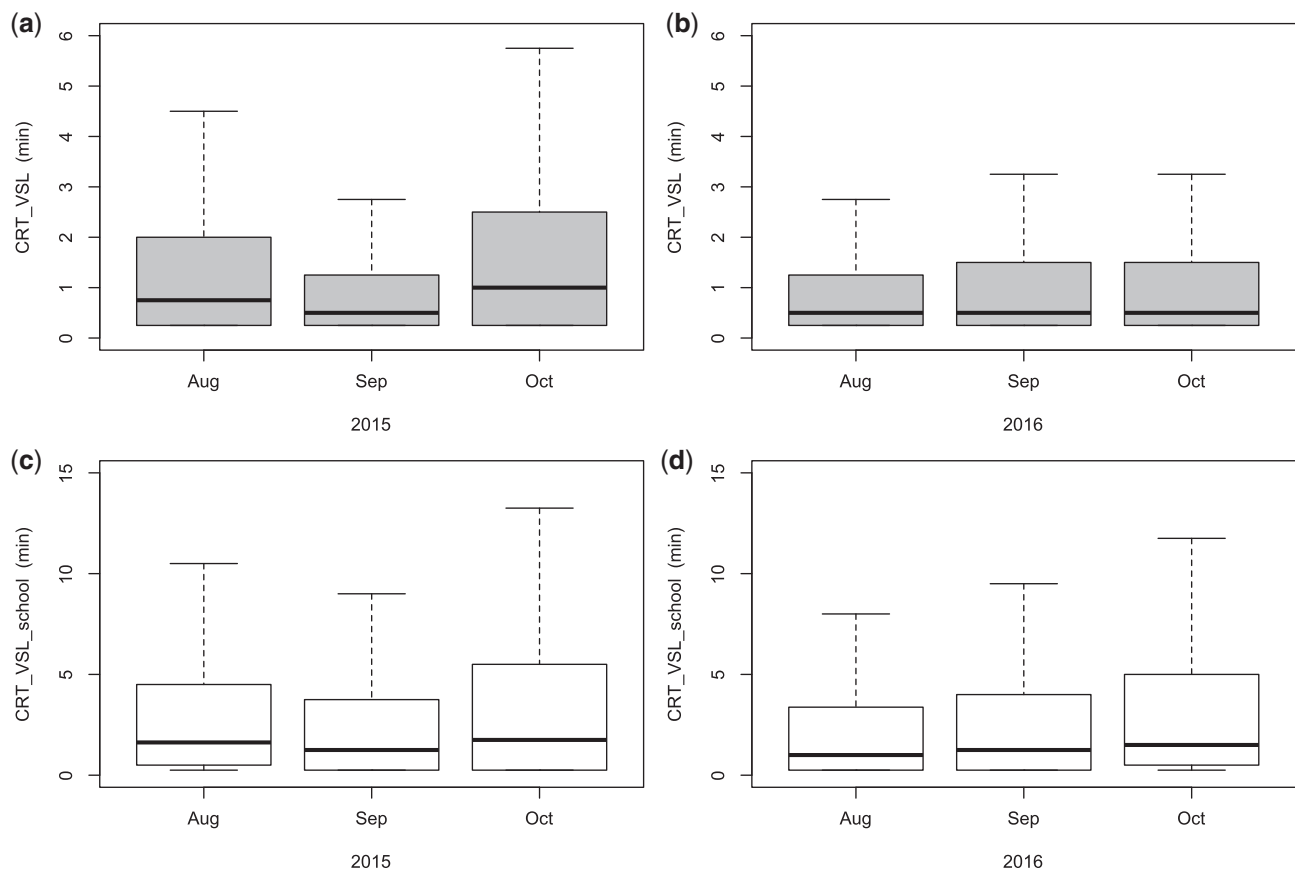


Figure 8. Boxplot of daytime CRT_{VSL} (top) recorded between August and October for 2015 (a) and 2016 (b) as well as the CRT_{VSL}^{school} (bottom) of the correspondent periods in 2015 (c) and 2016 (d). 2016 (right).

First, it demonstrated that 90% of the vertical positions sampled within a temporal window of 10 min around individual surfacing events were located within 0–20 m. Furthermore, we show a high correlation between the number of surfacing events (i.e. the

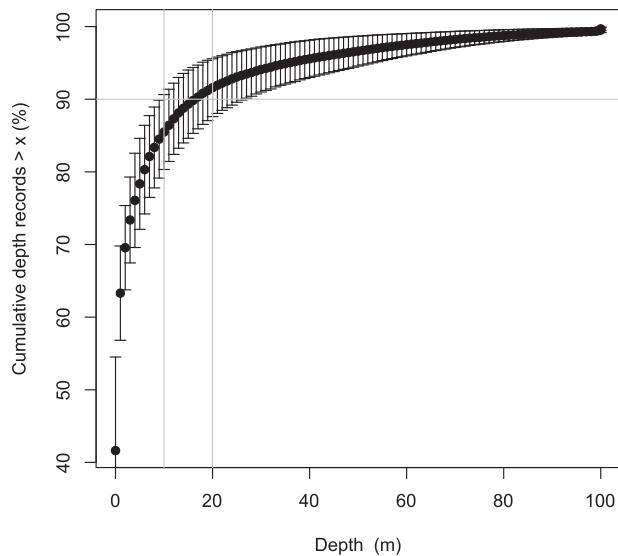


Figure 9. Cumulative curves of the depth records surrounding surface presence events (0–1 m) within a randomly allocated interval of 600 s based on the DepthTS from recovered tags.

number of CRT_{VSL}) and the residence times in the 0–20 m layer (CRT_{NSL}). The latter showed a decreasing trend in duration between summer and autumn. A similar decline was observed in the combined daily presence rates in the NSL of all tags and the thermal destratification of the water column. As such, the decrease in the surface availability of tuna from summer to autumn can be explained by means of residency in the 0–20 m layer (that affect the number of surfacing events) rather than by the continuous times spent in the 0–1 m layer. This implies that the time spent within this layer can provide a good proxy for the presence rates in the VSL. Moreover, lower-resolution depth time series obtained from transmitted data can already provide sufficient information to evaluate the actual surface availability of ABFT in the region. These results strengthen previous findings by [Bauer et al. \(2017\)](#) on ABFT and [Eveson et al. \(2018\)](#) on Southern bluefin tuna (SBFT) that used the time spent in the NSL as a proxy for the surface availability.

Accordingly, the apparent absence in temporal trends in the CRT_{VSL} (0–1 m) likely means that the presence of ABFT at the visible surface corresponds to instantaneous events, probably related to foraging activity. On the other hand, the temporal trends observed for the CRTs in the NSL (0–20 m) and DL (>20 m) may reflect the existence of two behavioural states (“near the surface” and “deep”), associated with two different feeding strategies of tuna, foraging at the surface and deeper as indicated earlier by [Bauer et al. \(2017\)](#). These behavioural states may be triggered by the seasonal oceanographic conditions that can affect the presence of forage at the surface ([Saraux et al., 2014](#)).

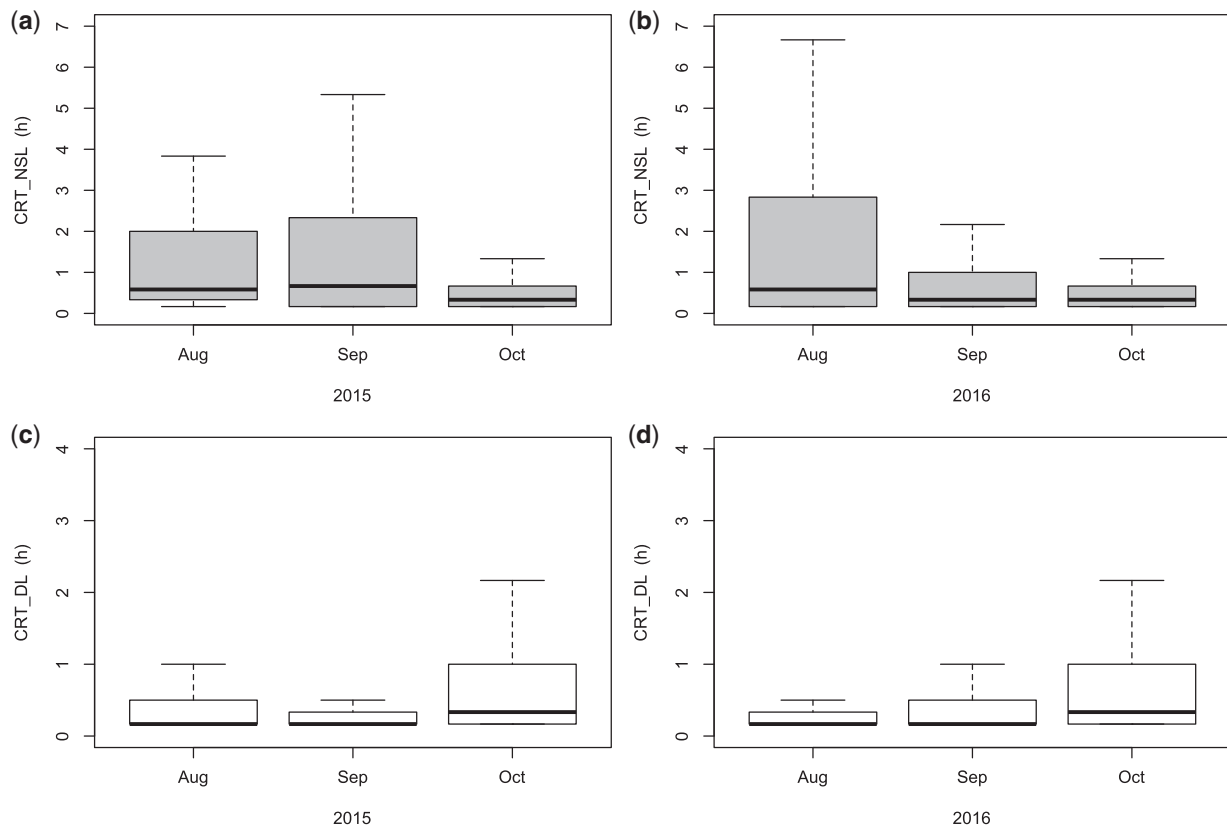


Figure 10. Boxplot of daytime CRT_{NSL} (top; 0–20 m) recorded between August and October for 2015 (a) and 2016 (b) as well as the daytime CRT_{DL} (bottom; >20 m) of the correspondent periods in 2015 (c) and 2016 (d).

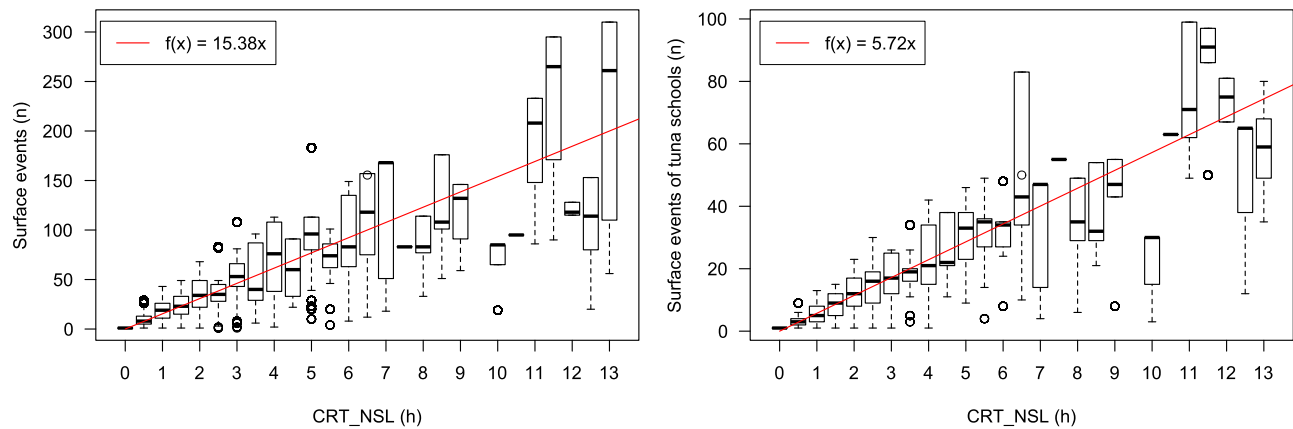


Figure 11. Relationship between the continuous residence times in the 0–20 m layer (CRT_{NSL}) during daytime of individual tunas to the number of surface events (left) and that of tuna schools (right). The red line indicates the correlation of the variables in both relationships, with the number of surface events being a function of the CRT_{NSL} durations.

Similarly, it is important to consider the habitat use and function when relating surface presence and surface-feeding activity. In nursery areas such as the Gulf of Lion and the Great Australian Bight, juvenile tuna schools are almost exclusively detected during surface foraging events while conducting aerial surveys (Bauer et al., 2015a; Eveson et al., 2018). In such areas, surface presence and feeding activity are therefore linked. In contrast in some regions, such as the “Tuna Alley” in the Great Bahama Banks (Lutcavage and Kraus, 1997), large adults are migrating at the surface presumed to be on their northerly migration and not actively engaged in feeding as ABFT in the Gulf of Lion (Bauer et al., 2015a). Therefore, in other regions, the relationship between surface activity and behaviour should be investigated further to identify those factors driving surface behaviour in those other regions. Other sensors incorporated into PSATs, such as accelerometers and sonars, could help to distinguish the different behaviours of ABFT and identify feeding events during surface presence periods (Jorgensen et al., 2015; Lawson et al., 2015). Such an application would further facilitate the quantification of surface-feeding events and their duration.

The apparent relation between a decline in the thermal stratification and different ABFT surface presence indicators has strong implications for ABFT aerial surveys, conducted in the same study area since 2000 (Bauer et al., 2015a). Derived ABFT abundance estimates are currently not corrected by their surface availability. Such a correction is of overall importance because a large fraction of survey repetitions is being conducted during the de-stratification period. In case of cetaceans, this is usually done by applying average (CRT) durations of surfacing and submergence (Bauer et al., 2015c). Similar approaches that account for the time spent by ABFT in the visible surface and its possible temporal and inter-individual variability should be incorporated in the derivation of the abundance indices for ABFT based on aerial surveys data. In this respect, further research directions could explore the use of empirical models that incorporate the vertical behaviour of ABFT schools based on the vertical dynamics found herein and provide the number of schools spotted at the sea surface along the aerial surveys transects. These models would allow evaluating the sensitivity and robustness of the abundance indices with respect to the inter-individual, daily and seasonal variability found herein. Moreover, they could allow testing the effectiveness

of different aerial survey sampling strategies (transect characteristics; number of surveys, temporal spread of the surveys). Finally, these models would allow standardizing the derived abundance indices accounting for the seasonal effects. In this respect, our results, in conjunction with external data on the thermal stratification in the Gulf of Lion (i.e. from future deployments of oceanographic data buoys or validated ocean models; Hu et al., 2009) will further help us to address these effects in upcoming or even past survey years.

Supplementary data

Supplementary material is available at the *ICESJMS* online version of the manuscript.

Acknowledgements

We thank the crews of the Cyngali and Roussillon Fishing recreational fishing vessels for their cooperation during the tagging cruises.

Funding

The study was part of the BLUEMED project and funded by the French National Research Agency (ANR; Project-ID ANR-14-ACHN-0002).

References

- Amante, C., and Eakins, B. W. 2009. ETOPO1 1 Arc-Minute Global Relief Model: Procedures, Data Sources and Analysis. NOAA Technical Memorandum NESDIS NGDC-24. 19 pp.
- Basson, M., and Farley, J. H. 2014. A standardised abundance index from commercial spotting data of southern bluefin tuna (*Thunnus maccoyii*): random effects to the rescue. *PLoS One*, 9: e116245.
- Bauer, R. 2018. RchivalTag: Analyzing Archival Tagging Data. R package version 0.0.8. <https://cran.r-project.org/package=RchivalTag> (last accessed 11 May 2020).
- Bauer, R. 2019. oceanmap: A Plotting Toolbox for 2D Oceanographic Data. R package version 0.1.0.1. <https://cran.r-project.org/package=oceanmap> (last accessed 11 May 2020).
- Bauer, R. K., Bonhommeau, S., Brisset, B., and Fromentin, J.-M. 2015a. Aerial surveys to monitor bluefin tuna abundance and track efficiency of management measures. *Marine Ecology Progress Series*, 534: 221–234.

- Bauer, R. K., Forget, F., and Fromentin, J. M. 2015b. Optimizing PAT data transmission: assessing the accuracy of temperature summary data to estimate environmental conditions. *Fisheries Oceanography*, 24: 533–539.
- Bauer, R. K., Fromentin, J.-M., Demarcq, H., and Bonhommeau, S. 2017. Habitat use, vertical and horizontal behaviour of Atlantic bluefin tuna (*Thunnus thynnus*) in the Northwestern Mediterranean Sea in relation to oceanographic conditions. *Deep Sea Research Part II: Topical Studies in Oceanography*, 141: 248–261.
- Bauer, R. K., Fromentin, J.-M., Demarcq, H., Brisset, B., and Bonhommeau, S. 2015c. Co-occurrence and habitat use of fin whales, striped dolphins and Atlantic bluefin tuna in the Northwestern Mediterranean Sea. *PLoS One*, 10: e0139218.
- Bonhommeau, S., Farrugio, H., Poisson, F., and Fromentin, J.-M. 2010. Aerial surveys of bluefin tuna in the western Mediterranean Sea: retrospective, prospective, perspectives. *Collective Volume of Scientific Papers ICCAT*, 65: 801–811.
- Brill, R., Lutcavage, M., Metzger, G., and Bushnell, P. 2002. Horizontal and vertical movements of juvenile bluefin tuna (*Thunnus thynnus*), in relation to oceanographic conditions of the western North Atlantic, determined with ultrasonic. *Fishery Bulletin*, 100: 155–167.
- Capello, M., Robert, M., Soria, M., Potin, G., Itano, D., Holland, K., Deneubourg, J. L., *et al.* 2015. A methodological framework to estimate the site fidelity of tagged animals using passive acoustic telemetry. *PLoS One*, 10: e0134002.
- Druon, J. N., Fromentin, J. M., Aulanier, F., and Heikkonen, J. 2011. Potential feeding and spawning habitats of Atlantic bluefin tuna in the Mediterranean Sea. *Marine Ecology Progress Series*, 439: 223–240.
- Eveson, J. P., Patterson, T. A., Hartog, J. R., and Evans, K. 2018. Modelling surfacing behaviour of southern bluefin tuna in the Great Australian Bight. *Deep-Sea Research Part II: Topical Studies in Oceanography*, 157–158: 179–189.
- Farley, J., and Ohshimo, S. 2018. Review and insights into the differences in reproductive parameter estimates between Eastern and Western Atlantic bluefin tuna stocks. *Collective Volume of Scientific Papers ICCAT*, 75: 1472–1493.
- Farrugio, H. 1977. Données préliminaires sur la pêche au thon rouge au filet tournant en Méditerranée française. *Collective Volume of Scientific Papers ICCAT*, 6: 245–252.
- Forsythe, G. E., Malcolm, M. A., and Moler, C. B. 1977. *Computer Methods for Mathematical Computations*. Prentice-Hall Series in Automatic Computation. Wiley, Prentice-Hall. 259 pp.
- Fromentin, J.-M. 2003. The East Atlantic and Mediterranean bluefin tuna stock management: uncertainties and alternatives. *Scientia Marina*, 67: 51–62.
- Fromentin, J.-M., Bonhommeau, S., Arrizabalaga, H., and Kell, L. T. 2014. The spectre of uncertainty in management of exploited fish stocks: the illustrative case of Atlantic bluefin tuna. *Marine Policy*, 47: 8–14.
- Fromentin, J.-M., and Lopuszanski, D. 2014. Migration, residency, and homing of bluefin tuna in the western Mediterranean Sea. *ICES Journal of Marine Science*, 71: 510–518.
- Fromentin, J.-M., and Powers, J. E. 2005. Atlantic bluefin tuna: population dynamics, ecology, fisheries and management. *Fish and Fisheries*, 6: 281–306.
- Galuardi, B., and Lutcavage, M. 2012. Dispersal routes and habitat utilization of juvenile Atlantic bluefin tuna, *Thunnus thynnus*, tracked with mini PSAT and archival tags. *PLoS One*, 7: e37829.
- Hu, Z., Doglioli, A., Petrenko, A., Marsaleix, P., and Dekeyser, I. 2009. Numerical simulations of eddies in the Gulf of Lion. *Ocean Modelling*, 28: 203–208.
- ICCAT. 2013. Report of the 2012 Atlantic Bluefin Tuna Stock Assessment Session. *Collective Volume of Scientific Papers ICCAT*, 69: 1–198.
- Jorgensen, S. J., Gleiss, A. C., Kanive, P. E., Chapple, T. K., Anderson, S. D., Ezcurra, J. M., Brandt, W. T., *et al.* 2015. In the belly of the beast: resolving stomach tag data to link temperature, acceleration and feeding in white sharks (*Carcharodon carcharias*). *Animal Biotelemetry*, 3: 10.
- Kitagawa, T., Kimura, S., Nakata, H., and Yamada, H. 2007. Why do young Pacific bluefin tuna repeatedly dive to depths through the thermocline? *Fisheries Science*, 73: 98–106.
- Lawson, G. L., Hückstädt, L. A., Lavery, A. C., Jaffré, F. M., Wiebe, P. H., Fincke, J. R., Crocker, D. E., *et al.* 2015. Development of an animal-borne “sonar tag” for quantifying prey availability: test deployments on northern elephant seals. *Animal Biotelemetry*, 3: 22.
- Lutcavage, M., and Kraus, S. 1997. Aerial survey of giant bluefin tuna, *Thunnus thynnus*, in the Great Bahama Bank, Straits of Florida, 1995. *Fishery Bulletin*, 95: 300–310.
- Lutcavage, M. E., Brill, R. W., Skomal, G. B., Chase, B. C., Goldstein, J. L., and Tutein, J. 2000. Tracking adult North Atlantic bluefin tuna (*Thunnus thynnus*) in the northwestern Atlantic using ultrasonic telemetry. *Marine Biology*, 137: 347–358.
- Marcek, B. J., Fabrizio, M. C., and Graves, J. E. 2016. Short-term habitat use of juvenile Atlantic bluefin tuna. *Marine and Coastal Fisheries*, 8: 395–403.
- R Core Team. 2017. R: A Language and Environment for Statistical Computing. R Foundation for Statistical Computing, Vienna, Austria. <https://www.r-project.org/> (last accessed 11 May 2020).
- Reynolds, R. W., Rayner, N. A., Smith, T. M., Stokes, D. C., and Wang, W. 2002. An improved *in situ* and satellite SST analysis for climate. *Journal of Climate*, 15: 1609–1625.
- Robert, M., Dagorn, L., Filmlalter, J. D., Deneubourg, J. L., Itano, D., and Holland, K. 2013. Intra-individual behavioral variability displayed by tuna at fish aggregating devices (FADs). *Marine Ecology Progress Series*, 484: 239–247.
- Royer, F., Fromentin, J.-M., and Gaspar, P. 2004. The association between bluefin tuna schools and oceanic features in the Western Mediterranean Sea. *Marine Ecology Progress Series*, 269: 249–263.
- Saraux, C., Fromentin, J.-M., Bigot, J. L., Bourdeix, J. H., Morfin, M., Roos, D., Van Beveren, E., *et al.* 2014. Spatial structure and distribution of small pelagic fish in the North-western Mediterranean Sea. *PLoS One*, 9: e111211.
- Service Argos Inc. 2005. Basic Description of the Argos System. Service Argos, Inc., Largo, MD. 7 pp.
- Venables, W. N., and Ripley, B. D. 2002. *Modern Applied Statistics with S*, 4th edn. Springer, New York.
- Walli, A., Teo, S. L. H., Boustany, A., Farwell, C. J., Williams, T., Dewar, H., Prince, E., *et al.* 2009. Seasonal movements, aggregations and diving behavior of Atlantic bluefin tuna (*Thunnus thynnus*) revealed with archival tags. *PLoS One*, 4: e6151.
- Wardle, C. S., Videler, J. J., Arimoto, T., Franco, J.-M., and He, P. 1989. The muscle twitch and the maximum swimming speed. *Journal of Fish Biology*, 35: 129–137.
- Wildlife Computers. 2015. Data Portal’s Location Processing (GPE3 & FastLoc-GPS) User Guide. Wildlife Computers, Redmond, WA. 25 pp.
- Wildlife Computers. 2016. MiniPAT User Guide. Wildlife Computers, Redmond, WA. 26 pp.

Handling editor: Jonathan Grabowski